Inorganic Chemistry

Article

pubs.acs.org/IC

Effect of Lanthanide Complex Structure on Cell Viability and Association

Katie L. Peterson, Jonathan V. Dang, Evan A. Weitz, Cutler Lewandowski, and Valérie C. Pierre*

Department of Chemistry, University of Minnesota, Minneapolis, Minnesota 55455, United States

Supporting Information

ABSTRACT: A systematic study of the effect of hydrophobicity and charge on the cell viability and cell association of lanthanide metal complexes is presented. The terbium luminescent probes feature a macrocyclic polyaminocarboxylate ligand (DOTA) in which the hydrophobicity of the antenna and that of the carboxyamide pendant arms are independently varied. Three sensitizing antennas were investigated in terms of their function in vitro: 2-methoxyisophthalamide (IAM(OMe)), 2-hydroxyisophthalamide (IAM), and 6-methylphenanthridine (Phen). Of these complexes, Tb-DOTA-IAM exhibited the highest quantum yield, although the higher cell viability and more facile synthesis of the structurally related Tb-DOTA-IAM(OMe) platform renders it more attractive. Further modification of this latter core structure with carboxyamide arms featuring hydrophobic benzyl, hexyl, and trifluoro groups as well as hydrophilic amino acid based moieties generated a family of complexes that exhibit high cell viability (ED_{50} > 300 μM) regardless of the lipophilicity or the overall complex charge. Only the hexyl-substituted complex reduced cell viability to 60% in the presence of 100 μM complex. Additionally, cellular association was investigated by ICP-MS and fluorescence microscopy. Surprisingly, the hydrophobic moieties did not increase cell association in comparison to the hydrophilic amino acid derivatives. It is thus postulated that the hydrophilic nature of the 2-methoxyisophthalamide antenna (IAM(OMe)) disfavors the cellular association of these complexes. As such, responsive luminescent probes based on this scaffold would be appropriate for the detection of extracellular species.

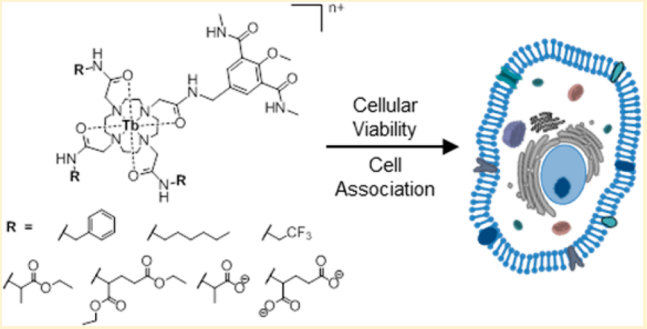

INTRODUCTION

Luminescent metal complexes are increasingly employed as biomolecular and cellular probes due to their unique photophysical properties that make them particularly well suited to monitor biological processes.[1] Examples include not only complexes of transition metals such as Pt, Ir, and Ru but also those that incorporate lanthanides, most commonly Eu and Tb.[1d,2] In particular, the long luminescence lifetime of the emitting metal mitigates the interference of background fluorescence originating from the biological sample. Moreover, since the large energy difference between the absorbing and emissive states of these complexes removes self-absorption issues, their luminescence signal intensity is proportional to their concentration over a wide range of values. With this in mind, lanthanide-based molecular probes have been applied to the detection of reactive oxygen species (ROS),[3] redox-active metals,[4] pH,[5] and intracellular analytes, such as ATP.[6] The continued applications of such metal-based luminescent probes, however, further rely on the ability to limit their cellular association altogether for certain tissue imaging experiments or, alternatively, to direct them to specific cellular regions. Prior studies indicate that structural properties of metal complexes, such as their hydrophobicity and size, influence their cell viability and cellular association, including their membrane permeability.[7] Although cell-penetrating peptides have been applied to increase the cell uptake of lanthanide complexes,[8] the goal of this project is to modify the intrinsic properties of the metal complex to control cellular association. Presented here is a systematic study to evaluate the effects of structural variations on a core structure common to most luminescent lanthanide probes and an investigation of the practicality of such probes for cellular and tissue applications requiring extracellular imaging agents.

The most common platform of luminescent lanthanide complexes features a chelating polyaminocarboxylate ligand substituted with one or more carboxamide pendant arms from which additional moieties are attached, notably the probe's antenna. The Laporte-forbidden nature of the f−f transition dictates that, for practical applications in biologically relevant settings, the probe must incorporate a sensitizing antenna. In terms of the design of a responsive probe, the luminescence intensity of the lanthanide complex can then be modulated by altering, among other parameters, the excited triplet state energy level of the antenna and the antenna−lanthanide distance.[2a] For biological applications, it is thus important to

Received: February 4, 2014
Published: June 5, 2014

dx.doi.org/10.1021/ic500282n | Inorg. Chem. 2014, 53, 6013−6021

select an antenna with suitable energetic properties for lanthanide sensitization that is also resistant to quenching by the medium. Work by Parker and co-workers identified that the nature of the antenna, specifically its point of attachment to the cyclen backbone of the ligand, affects the subcellular localization of the complexes.[7d] This work focused primarily on azaxanthone and other extended aromatic antenna.[7c−e,9] Given the increasing use of phenanthridine and isophthalamide antennas for the design of luminescent lanthanide probes,[6,10] a deeper understanding of the structural parameters influencing their effect on cellular viability and cell association is necessary to further optimize their structures for biological application both extra- and intracellularly. Herein, two parameters were evaluated for their effect on cell viability and association: the nature of the antenna and that of the pendant amide arms.

Each complex features a luminescent Tb^{3+} ion chelated by a DOTA(m)-type ligand. The macrocyclic polyaminocarboxylate ligand provides kinetic inertness and thus predicted lower toxicity on cell viability.[11] Furthermore, the overall positively charged lanthanide complexes of DOTA tetraamide (DOTAm) ligands are kinetically more inert than the DOTA analogues as a result of the decreased basicity of the nitrogen atoms.[12] Moreover, the macrocyclic framework is less susceptible to enzymatic degradation.[12,13] The high kinetic inertness of macrocyclic lanthanide complexes and their ability to resist degradation is critical for their use in vivo. Three different antennas were investigated: the hydrophilic 2-hydroxyisophthalamide (IAM), a reported sensitizer of both Tb and Eu,[10c,d] the closely related and synthetically more facile 2-methoxyisophthalamide (IAM(OMe)), and the extended aromatic 6-methylphenanthridine (Phen) (Chart 1). For each

Chart 1. Chemical Structures of Tb-DOTA-IAM(OMe) ([Tb-1]), Tb-DOTA-IAM ([Tb-2]$^-$), and Tb-DOTA-Phen ([Tb-3])

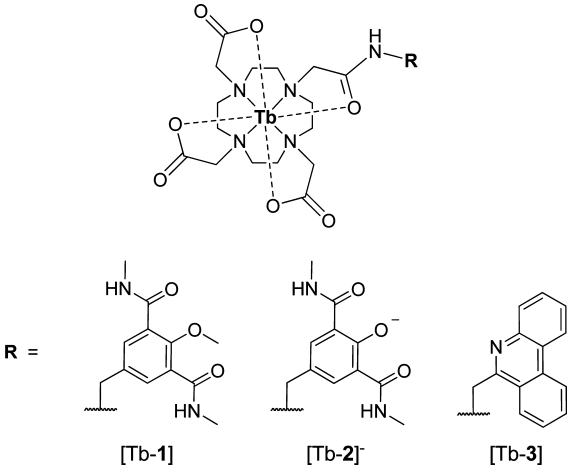

complex, the quantum yield, cellular viability, and cell association were evaluated. The effect of charge and hydrophobicity on cell viability and association was subsequently evaluated with complexes comprising the IAM(OMe) antenna functionalized with varying carboxamide arms (Chart 2).

RESULTS AND DISCUSSION

Synthesis of Lanthanide Complexes. The isophthalamide complexes Tb-DOTA-IAM(OMe) ([Tb-1]) and Tb-DOTA-IAM ([Tb-2]$^-$) were synthesized according to Scheme

Chart 2. Chemical Structures of Derivatives of [Tb-1] with Varying Charged and Hydrophobicities[a]

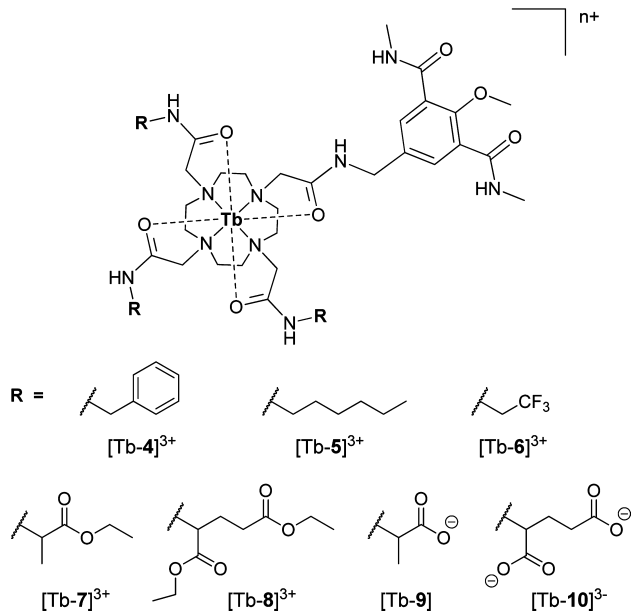

[a]All modifications were performed on the pendant arm.

1. Briefly, the oxidation of bis(hydroxymethyl)-*p*-cresol with MnO_2 and KOH generated the diacid **11**. Subsequent treatment with methyl iodide generated the methoxy-protected diester **12**, which was then converted to the diamide **13** with methylamine. The aldehyde **14** was generated via a Riley oxidation of the aryl methyl group in naphthalene at 215 °C. Periodinane oxidation methods (Dess−Martin and 2-iodoxybenzoic acid), permananganates, and chromates (Jones' reagent and PCC) were unsuccessful mediators of this transformation. Reaction of the aldehyde **14** with hydroxylamine hydrochloride generated the oxime **15**, which was crystallized by addition of diethyl ether to an acidic solution of the crude reaction mixture in ethyl acetate and methanol and then reduced to the amine form of the IAM antenna **16**. The tris-BOC-protected cyclen **17** was synthesized as reported[14] and further coupled to the amine **16** using HATU as the activating agent. BOC deprotection in a hydrochloric acid/methanol mixture afforded the IAM(OMe) cyclen conjugate **19**, which served as a common intermediate in the synthesis of complexes [Tb-**1**], [Tb-**2**]$^-$, and [Tb-**4**]$^{3+}$−[Tb-**10**]$^{3-}$.

Alkylation of the cyclen derivative **19** with *tert*-butyl bromoacetate yielded the protected ligand **20** (Scheme 1). Deprotection in a hydrochloric acid/methanol mixture yielded the free ligand DOTA-IAM(OMe) (**1**). Harsher deprotection conditions with boron tribromide removed both the *tert*-butyl groups and the aryl methyl ether to yield DOTA-IAM (**2**). The final complexes [Tb-**1**] and [Tb-**2**]$^-$ were obtained from their respective ligands, **1** and **2**, by heating with $TbCl_3$ in aqueous solutions at neutral to slightly basic pH for 2 days or more.[15] The phenathridine complex [Tb-**3**] was synthesized according to the published procedure.[6,10a]

In order to evaluate the role of charge and hydrophobicity of the lanthanide complex in its cellular compatibility, seven derivatives of Tb-DOTA-IAM(OMe) ([Tb-**1**]) were synthesized (Chart 2 and Scheme 1). The synthesis was designed to take advantage of the common intermediate **19**, described above. Each bromoacetamide arm was synthesized using a

dx.doi.org/10.1021/ic500282n | Inorg. Chem. 2014, 53, 6013−6021

Scheme 1. Synthesis of Tb-DOTA-IAM(OMe) ([Tb-1]), Tb-DOTA-IAM ([Tb-2]$^-$), and Tb-DOTA-IAM(OMe) Complexes with Varying Charge and Hydrophobicity ([Tb-4]$^{3+}$–[Tb-10]$^{3-}$)[a]

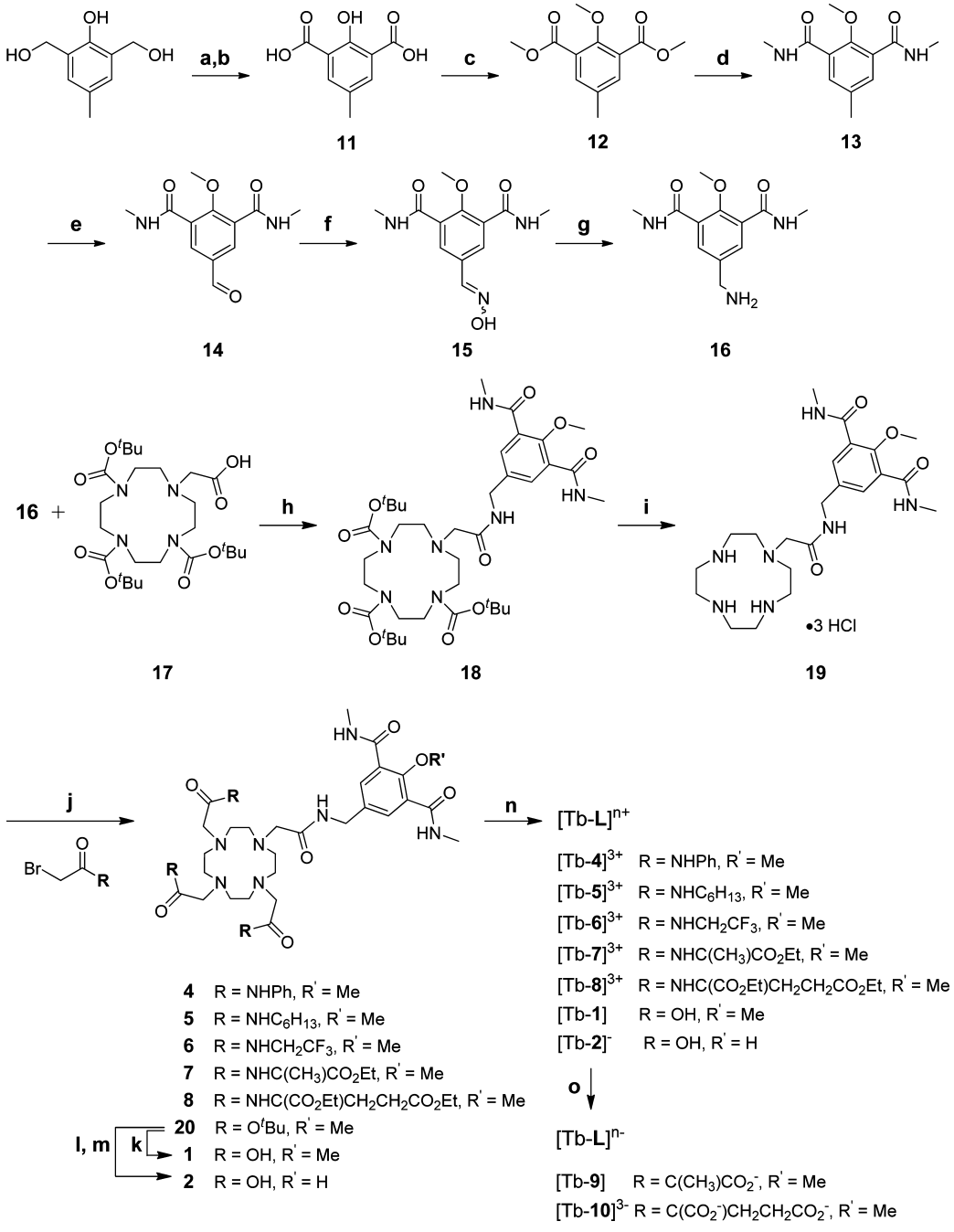

[a]Reagents and conditions: (a) MnO_2, CH_3Cl, 60 °C, 20 h; (b) KOH (s), 230 °C, 1 h; (c) CH_3I, K_2CO_3, acetone, 56 °C, 16 h; (d) NH_2CH_3, CH_3OH, 65 °C, 18 h; (e) SeO_2, naphthalene, 215 °C, 2.5 h; (f) hydroxylamine hydrochloride, pyridine, 22 °C, 24 h; (g) Pd/C (10%), HCl, ethanol/H_2O, 5 bar, 16 h; (h) HATU, DIPEA, DMF, 22 °C, 40 h; (i) HCl, CH_3OH, 22 °C, 18 h; (j) Cs_2CO_3, CH_3CN, 40 °C, 18 h; (k) HCl, CH_3OH, 22 °C, 18 h; (l) BBr_3, CH_2Cl_2, 25 °C, 18 h; (m) CH_3OH, 65 °C, 16 h; (n) $TbCl_3$, H_2O/CH_3OH, pH 7, 45 °C, 48 h; (o) 0.2 M KOH, H_2O, 22 °C, 20 h.

biphasic method in which bromoacetyl bromide in dichloromethane and aqueous potassium carbonate were simultaneously added dropwise to a solution of the corresponding amine in dichloromethane at 0 °C. This method resulted in moderate to high yields (65–85%) of the desired products in high purity. The ligands were obtained upon reaction of the bromoacetamide arms with the intermediate **19**. Metalation with $TbCl_3$ at neutral pH yielded [Tb-**4**]$^{3+}$–[Tb-**8**]$^{3+}$. The carboxylic acid derivatives [Tb-**9**] and [Tb-**10**]$^{3-}$ were obtained by saponification of their corresponding esters [Tb-**7**]$^{3+}$ and [Tb-**8**]$^{3+}$, respectively. Synthetic details and characterizations are given in the Supporting Information.

Quantum Yield and Quenching in Cell Lysate. The nature of the sensitizing antenna of a lanthanide complex can affect its function in a biological environment. Here, we compare [Tb-**1**], [Tb-**2**]$^-$, and [Tb-**3**], three complexes that

dx.doi.org/10.1021/ic500282n | Inorg. Chem. 2014, 53, 6013–6021

feature either an isophthalamide- or phenanthridine-based antenna for sensitizing the lanthanide emissions (Chart 1). Note that each complex has the same acetate pendant arms. All three complexes luminesce in the green region of the visible spectrum, with maximum emission at 545 nm upon excitation at 350 nm (Figure S1 (Supporting Information)). These three antenna platforms have different properties in terms of hydrophobicity and interactions with biomolecules, including nucleic acids, reducing agents, and proteins. The hydrophilic isophthalamide and methoxyisophthalamide are composed of a single aromatic ring and have no known interactions with biomolecules, while the phenanthridine is an extended aromatic system capable of base stacking with nucleotides and DNA intercalation.[6,10a]

The quantum yield, Φ, of the three Tb complexes in PBS was investigated by comparing the luminescence intensity of each complex to that of a quinine sulfate standard in 0.1 M sulfuric acid ($\Phi_r = 0.577$)[16] according to the optically dilute method.[10d] At pH 7.8 and 22 °C, the quantum yields of [Tb-**1**] and [Tb-**3**] are statistically identical (4.6 ± 1.2% vs 4.7 ± 2.2%, respectively). The quantum yield of the phenathridine derivative [Tb-**3**] is comparable to that of similar complexes featuring either triamide- or triphosphinate-substituted DOTA ligands.[17] However, $[Tb\text{-}\mathbf{2}]^-$ is a more efficient emitter with an average quantum yield of 9.8 ± 1.5%, indicating that substituting the methoxy for the hydroxyl group on the isophthalamide antenna substantially affects the quantum yield of the complex. Note that quantum yields of ca. 50% have been reported by Raymond and co-workers for Tb complexes with tetra-IAM-substituted ligands.[10d] The substantial difference between these complexes results from their structures. In contrast with the case for $[Tb\text{-}\mathbf{2}]^-$, in the tetra-IAM complex H(2,2)-IAM the isophthalamide directly coordinates the lanthanide, thereby enabling a Dexter-type energy transfer from the antenna to the Tb that is much more efficient than the Förster-type, through-space mechanism likely taking place in $[Tb\text{-}\mathbf{2}]^-$. On the other hand, $[Tb\text{-}\mathbf{2}]^-$ has substantially higher water solubility (M range) than the cryptand H(2,2)-IAM (μM range) and enables the design of responsive probes.

Nonetheless, the quantum yields of [Tb-**1**], $[Tb\text{-}\mathbf{2}]^-$, and [Tb-**3**] are comparable to those of luminescent d-block compounds used for cellular imaging. For example, the quantum yields of Ir complexes featuring 2-phenylpyridine ligands are between 4 and 8% in PBS buffer.[18] Not surprisingly, the quantum yields of Tb-centered luminescence are lower than those of commonly used fluorescence dyes such as Cy3 (4% in PBS), Cy5 (30% in PBS), Alexa750 (12% in phosphate buffer), and Texas Red (30% in water).[19] However, in comparison with phosphorescent metal complexes, organic dyes suffer from short fluorescence lifetimes and small Stokes shifts.[20]

As for any luminescent or fluorescent probe, emission is susceptible to quenching by reducing agents, proteins, and other components of biological media. In the case of luminescent Tb and Eu complexes, the quenching pathways can involve electron or charge transfer from the excited states to intracellular reducing agents such as urate, ascorbate, and glutathione that are present in mM concentrations in cells.[21] In addition, luminescence quenching by proteins, such as human serum albumin, has been reported.[22] The degree of luminescence quenching was evaluated by measuring the time-delayed luminescence intensity of [Tb-**1**] with respect to its concentration in PBS and whole cell lysate at two different protein concentrations. In whole cell lysate containing 0.25 mg of protein/mL, the luminescence intensity of [Tb-**1**] is quenched by 22 ± 2.8%; at 0.5 mg of protein/mL the luminescence intensity is reduced by 30 ± 2.4% (Table 1 and Figure S2 (Supporting Information)). Advantageously, the isophthalamide antenna is less susceptible to quenching than complexes containing electron-poor sensitizing moieties. For instance, the metal-centered emission of terbium azaxanthone complexes is quenched by 30−60% in the presence of 0.2 mM human serum albumin.[22] This highlights the potential of the IAM(OMe) antenna for biological applications.

Table 1. Luminescence Quenching of [Tb-1] by Whole Cell Lysate[a]

concn, mg of protein/mL	quenching (%)[b]
0.25	22 ± 2.8
0.50	30 ± 2.4

[a]Experimental conditions: [Tb-**1**] = 0−15 μM, PBS, pH 7.8, time delay 0.1 ms, excitation wavelength 345 nm, slit widths (excitation and emission) 5 nm, integrated emission intensity from 470 to 635 nm, T = 20 °C. Results are mean ± SD (n = 3). Whole cell lysate was generated from L6 myoblasts; the protein concentration was determined by a BCA assay. [b]Percent quenching was calculated using the percent change in the slope of the integrated luminescence intensity versus the [Tb-**1**] (μM) plots (Figure S2 (Supporting Information)).

Influence of the Nature of the Antenna on Cellular Compatibility. The effect of [Tb-**1**], $[Tb\text{-}\mathbf{2}]^-$, and [Tb-**3**] on the viability of L6 rat muscle myoblast cells was investigated using an MTT assay. It was hypothesized that the 2-methoxyisophthalamide would have a reduced effect on cell viability due to the protecting group on the phenol that could block nonspecific interactions with the cell proteins and coordination of cellular metals, such as iron and copper. Additionally, the phenathridine complex [Tb-**3**] was expected to have a greater effect on cell viability due to its ability to intercalate DNA and RNA.[10a,23] Following a 24 h incubation with 0−300 μM Tb complex, the phenanthridine derivative [Tb-**3**] decreased cell viability to 74% at 100 μM and to 63% at 300 μM. On the other hand, the cellular viability was maintained at or above 80% for both isophthalamide complexes [Tb-**1**] and $[Tb\text{-}\mathbf{2}]^-$ (Table 2 and Figure 1). The similar profiles indicate that the methoxy protecting group on the isophthalamide does not significantly improve cell viability at the doses studied here. This is in contrast to a pair of Rh probes chelated by chrysenequinone diimine and *N*-functionalized dipyridylamine ligands, for which small structural changes were shown to have a substantial impact on cell viability. In that case, altering the ethanol substituent to a propyl reduces the viability of HCT116N and HCT116O cells from 80% to 60% after a 24 h incubation with 40 μM complex.[7b]

Overall, the complexes in this study influence cell viability slightly less than complexes containing tetraazatriphenylene or azaxanthone antennas with phenyl or ethyl ester substituted carboxamide arms, which have ED_{50} values in the 100 μM to >240 μM range.[7d,e,24] They affect cell viability similarly to Ru(III) polypyridine complexes, which also have ED_{50} (72 h) values ≥300 μM in MCF-7 and HT-29 cell lines.[25] It is interesting to note that the europium compound of 1,4,7,10-tetraazacyclododecane-1,4,7,10-tetraacetic acid containing no antenna moiety, $[Eu\text{-}DOTA]^-$, has a negligible effect on cell viability from 0 to 500 μM with a 72 h incubation.[26] Thus, with

dx.doi.org/10.1021/ic500282n | Inorg. Chem. 2014, 53, 6013−6021

Table 2. Cellular Viability and Association of Macrocyclic Tb Complexes

	cell viability[a] (%)	cell association[b] (μmol of Tb/g of protein)
[Tb-**1**]	96 ± 6	6.0 ± 3
[Tb-**2**]$^-$	80 ± 3	12 ± 5
[Tb-**3**]	74 ± 9	5.3 ± 3
[Tb-**4**]$^{3+}$	81 ± 2	1.4 ± 0.6
[Tb-**5**]$^{3+}$	63 ± 4	22 ± 10
[Tb-**6**]$^{3+}$	90 ± 8	8.3 ± 3
[Tb-**7**]$^{3+}$	78 ± 8	2.2 ± 0.5
[Tb-**8**]$^{3+}$	90 ± 6	0.32 ± 0.07
[Tb-**9**]	81 ± 4	1.3 ± 0.4
[Tb-**10**]$^{3-}$	88 ± 10	0.47 ± 0.2
control (no Tb complex)	100 ± 6	0.07 ± 0.04

[a]Obtained by an MTT assay after a 24 h incubation with 100 μM complex. Results are mean ± SD (n = 3). [b]Determined by ICP-MS after a 4 h incubation with 50 μM complex. Results are mean ± SD (n = 3).

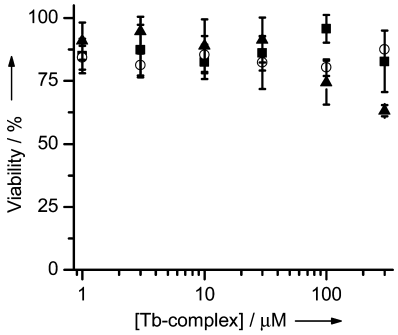

Figure 1. Viability (24 h) of L6 myoblasts treated with 0−300 μM [Tb-**1**] (solid squares), [Tb-**2**]$^-$ (open circles), and [Tb-**3**] (solid triangles) as determined with an MTT assay. Results are expressed as mean ± SD (n = 3).

respect to cell viability, [Tb-**1**] and [Tb-**2**]$^-$ are preferred for cellular imaging applications compared to [Tb-**3**].

The nature of the antenna was also expected to affect the cellular association of the complexes. Following a 4 h incubation with 50 μM of Tb complex, the cellular accumulation of the metal was determined by ICP-MS and expressed relative to the protein concentration as determined by a BCA assay. Importantly, it should be noted that the quantitative nature of measuring cellular association of metal complexes by ICP-MS is balanced by the inability of the technique to distinguish between internalized or membrane-bound complexes.[27] It was anticipated that the extended aromatic antenna of [Tb-**3**] would facilitate membrane permeability, as suggested by the increased cellular uptake of more lipophilic Ru complexes and phenanthridine-substituted cisplatin.[7a,27,28] However, the cell association values of the hydrophilic Tb-DOTA-IAM(OMe) ([Tb-**1**]) and Tb-DOTA-IAM ([Tb-**2**]$^-$) are statistically not different from the values for the hydrophobic Tb-DOTA-Phen ([Tb-**3**]) (Table 2).

Small structural changes to the ligands of metal complexes have been reported to exert varied effects on the intracellular accumulation and distribution. Using a group of lanthanide complexes with tetraazatriphenylene- or azaxanthone-based antennas, Parker identified that how the antenna was linked to the cyclen ring affected membrane permeability and localization more than small structural modifications on the antenna itself.[7d] For the isophthalamide complexes, however, conversion from the methoxy group in [Tb-**1**] to the phenolate of [Tb-**2**]$^-$ does affect cellular association. This observation is more in concert with the findings of Barton, who measured substantial differences in cell association between an alkyl-substituted dipyridyl Rh complex (705 ng of Rh/mg of protein) in comparison to a complex that introduced a terminal alcohol on the alkyl group (165 ng of Rh/mg of protein).[7b] The cellular association values measured for the hydroxyisophthalamide [Tb-**2**]$^-$ are comparable to the values reported for a Tb complex with a tetraazatriphenylene antenna and phenyl-substituted amide arms, which had a maximum accumulation of 10 μmol/g of protein into NIH 3T3 cells after a 4 h incubation at 50 μM.[7d] Unfortunately, further comparisons with cellular accumulation values reported in the literature are limited due to differences in the method of data collection (ICP-MS vs flow cytometry[7a,21a,29]), and data presentation of metal per amount of protein or per cell.[7e,24,25,28,30]

Notable differences among the three metal complexes include the increased effect of [Tb-**3**] on cell viability above 100 μM in spite of its only modest cell association. The synthesis of [Tb-**2**]$^-$ requires a synthetically challenging boron tribromide deprotection to produce the 2-hydroxyisophthalamide antenna, and the resulting complex has a cellular association only slightly higher than that of its analogue [Tb-**1**]. The more facile synthesis of the 2-methoxyisophthalamide of [Tb-**1**] in comparison to [Tb-**2**]$^-$ thus became a significant

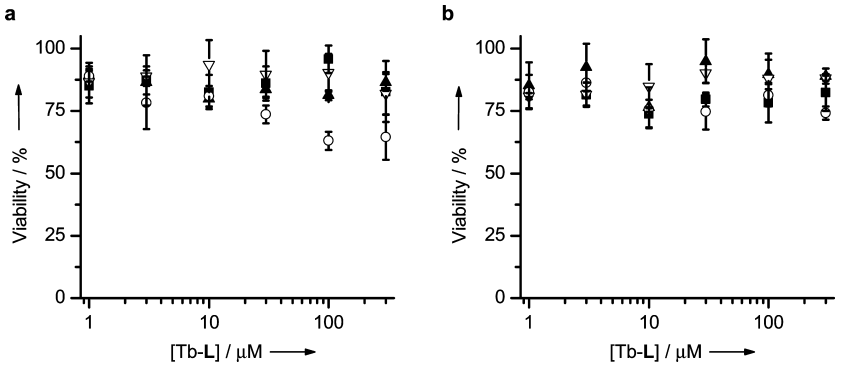

Figure 2. Viability (24 h) of L6 myoblasts treated with 0−300 μM Tb complexes as determined with an MTT assay: (a) [Tb-**1**] (solid squares), [Tb-**4**]$^{3+}$ (solid triangles), [Tb-**5**]$^{3+}$ (open circles), and [Tb-**6**]$^{3+}$ (open inverted triangles); (b) [Tb-**7**]$^{3+}$ (solid squares), [Tb-**8**]$^{3+}$ (solid triangles), [Tb-**9**] (open circles), and [Tb-**10**]$^{3-}$ (open inverted triangles). Results are expressed as mean ± SD (n = 3).

dx.doi.org/10.1021/ic500282n | Inorg. Chem. 2014, 53, 6013−6021

factor in selecting an antenna for further studies evaluating the effects of variable arms on the cellular compatibility of lanthanide complexes.

Effect of Structural and Electronic Variations in Pendant Arms on Cell Viability and Association. The role of charge and hydrophobicity of the polyaminocarboxylate arms on the cell viability and association of the lanthanide probes was evaluated with a library of derivatives of [Tb-**1**]. Complexes [Tb-**4**]$^{3+}$−[Tb-**10**]$^{3-}$ share a common cyclen backbone with a 2-methoxyisophthalamide antenna but differ in the nature of the remaining substituents (Chart 2). The alkyl, benzyl, and trifluoro groups impart increasing hydrophobicity to the complexes, whereas alanine and glutamine amino acid based substituents in either an ethyl ester or carboxylic acid form render greater hydrophilicity. The resulting complexes also differ in overall complex charge; neutral carboxamide arms generate the 3+ charged complexes [Tb-**4**]$^{3+}$−[Tb-**8**]$^{3+}$, the addition of monoanionic arms forms the zwitterionic complex [Tb-**9**], and the dianionic glutamate arm creates [Tb-**10**]$^{3-}$ bearing a net 3− charge.

As with the previous complexes that differ with respect to the antenna, the cell viability (24 h) was measured for the library of complexes featuring pendant arms with structural and electronic variations. Of the hydrophobic complexes, only [Tb-**5**]$^{3+}$ decreases cell viability significantly to 60%, while the values for [Tb-**4**]$^{3+}$ and [Tb-**6**]$^{3+}$ are comparable to that of the parent complex [Tb-**1**], maintaining a viability above 80% in the concentration range measured (Figure 2a and Table 2). Each of the amino acid derivatives [Tb-**7**]$^{3+}$, [Tb-**8**]$^{3+}$, [Tb-**9**], and [Tb-**10**]$^{3-}$ also sustain viability above 75% even in the presence of 300 μM Tb complex (Figure 2b and Table 2). Interestingly, the notable reduction in cell viability upon addition of medium-length alkyl chains matches the results of a previous study comparing a family of Ir(III) cyclometalated probes. In that study, the Ir complexes featuring the shortest (C_2) and longest (C_{18}) alkyl chains had comparably minimal effects on HeLa cell viability ($ED_{50} \approx 15$ μM), while the median length alkyl chain (C_{10}) was significantly more cytotoxic ($ED_{50} = 2$ μM).[29b] The hexyl alkyl derivative [Tb-**5**]$^{3+}$ excluded, the relatively low effect on cell viability (ED_{50} values >300 μM) of this entire class of Tb complexes suggests they have only limited interactions with cellular components and bodes well for their application.

The role of the pendant arms on the cellular association of the Tb complexes was also investigated by ICP-MS. It was hypothesized, on the basis of the results of Barton,[7a,27] that [Tb-**4**]$^{3+}$, [Tb-**5**]$^{3+}$, and [Tb-**6**]$^{3+}$ would penetrate cells more efficiently due to their lipophilic substituents and cationic character that would assist transport across the membrane.[31] Indeed, higher Tb accumulation is observed with the hydrophobic hexyl-substituted [Tb-**5**]$^{3+}$ and trifluoro-containing [Tb-**6**]$^{3+}$ than with the more hydrophilic amino acid derivatives (Table 2). However, this conclusion cannot be universally applied to all hydrophobic arms, since the cellular association of the benzyl-substituted [Tb-**4**]$^{3+}$ is less than that of the parent complex [Tb-**1**]. The alkyl-substituted Ir complexes discussed previously also do not illustrate a direct relationship between hydrophobicity and cellular association. In that study, each complex investigated displayed measurable cellular association by ICP-MS, but the C_{10} version afforded the greatest association, followed by the C_2 and then the C_{18} derivative.[29b] Thus, it is clear that the lipophilicity of the complex alone cannot be used to predict the cellular association of metal complexes.

Of the amino acid derivatized complexes, the alanine-based [Tb-**7**]$^{3+}$ and [Tb-**9**] have higher cell association values than the glutamine-based compounds [Tb-**8**]$^{3+}$ and [Tb-**10**]$^{3-}$. Positively charged complexes containing esters are reported to have enhanced cell association in comparison to carboxylic acid derivatives,[7a] and this is observed with the slightly higher cell association values of the ethyl ester complex of alanine [Tb-**7**]$^{3+}$ in comparison to the neutral acid complex [Tb-**9**]. This reflects the finding that the cell association of [Eu-DOTAm]$^{3+}$ is 5 times that of [Eu-DOTA]$^{-}$, which showed negligible cellular accumulation.[26] Interestingly, this trend is not repeated for the glutamine ethyl ester and acid complexes, [Tb-**8**]$^{3+}$ and [Tb-**10**]$^{3-}$, respectively, which both have low cell association values despite their large differences in overall complex charge. This is in contrast with to lanthanide complexes studied by Parker in which the intracellular concentration of a 3− charged glutamate-functionalized DOTA with a tetraazatriphenylene antenna was approximately 3 times that of the neutral Ln-DOTA-tetraazatriphenylene.[21a] An important conclusion is that the parameters influencing cellular association of lanthanide complexes are multifaceted and include both structural features (lipophilicity, nature of the antenna, terminal functional groups) and, to a lesser extent, overall complex charge.

This study investigated the effect of structural modifications of the ligand on cell association in the absence of targeting moieties; however, conjugating Ln complexes to cell-penetrating peptides[32] or receptor targeting groups has successfully increased the cellular uptake. Progress in the field of cell-penetrating, lanthanide-based contrast agents has been reviewed[8,33] and includes the use of polyarginine[34] and Tat-based peptides.[35] This technique has also been applied to luminescent metal complexes[36] and dual imaging agents.[37] Additional approaches to increase cellular accumulation include coupling complexes to moieties that facilitate interactions with cellular membrane receptors,[38] transporters,[39] or special groups such as exofacial thiols.[40] The translation of these approaches to the luminescent macrocyclic polyaminocarboxylate complexes described herein is being further investigated by our group.

Fluorescence Microscopy. The cellular association of the Tb complexes was also investigated with epifluorescence microscopy. L6 myoblasts were treated with Tb complex (200 μM for 4 h), washed with PBS at room temperature, and fixed with formaldehyde prior to imaging. Results of representative cells indicate the presence of weak cellular association for the trifluoro-substituted [Tb-**6**]$^{3+}$, while the fluorescence intensity of phenanthridine-containing [Tb-**3**] is comparable to that of the control cells (Figure 3). The remaining Tb complexes exhibit similar weak cellular fluorescence (Figure S3 (Supporting Information)). Due to reports that different staining patterns can be observed in experiments that differ only in whether cells were imaged in a live or fixed state,[41] the cellular association of [Tb-**6**]$^{3+}$ was also examined in live cells via fluorescence microscopy (Figure S4 (Supporting Information)). In these images, an overall decrease in the fluorescence to levels comparable to those for the untreated control cells was observed.

The reduced punctate staining in live cells in comparison to fixed cells has also been observed by Belitsky.[41] However, unlike our 2-hydroxyisophthalamide complexes, lanthanide complexes featuring tetraazatriphenylene antennas containing phenyl, ester, or carboxylate substituents are taken up by CHO

dx.doi.org/10.1021/ic500282n | Inorg. Chem. 2014, 53, 6013−6021

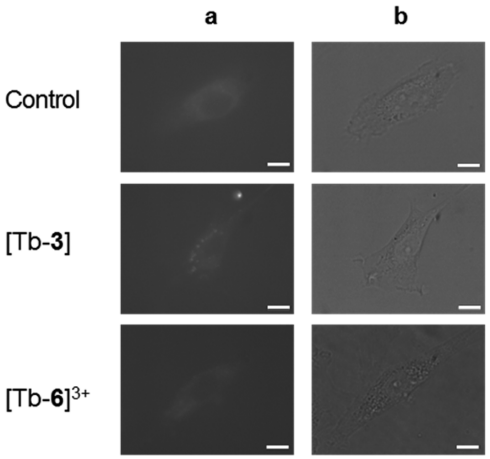

Figure 3. Fluorescence microscopy images of representative L6 myoblasts treated with 200 μM [Tb-**3**] and [Tb-**6**] for 4 h at 37 °C: (a) fluorescence images, 60× objective, 325−375 nm excitation filter, 470−750 nm emission filter, 0.4 s exposure time; (b) bright field images, 0.04 s exposure time. Cells were rinsed with PBS and fixed with formaldehyde prior to imaging. Scale bars represent 10 μm.

or NIH 3T3 cells and can be visualized with fluorescence microscopy regardless of the nature of their pendent arms.[7d] Likewise, Bünzli observed lanthanide helicates ranging in overall charge from 6− to 6+ localized to endosomes and lysosomes, consistent with endocytotic uptake mechanisms irrespective of the polarity or overall charge of the complex.[7c] Regardless of the reasons, the low cell associations exhibited by this entire class of complexes render them particularly useful for monitoring extracellular species.

CONCLUSIONS

A family of luminescent lanthanide complexes featuring different sensitizing antennas varying in charge and hydrophobicity and pendant arms of variable structural and electronic properties were synthesized. The cell viability and association of this family of complexes have been evaluated. With respect to the antenna, the 2-methoxyisophthalamide of [Tb-**1**] was selected as the ideal candidate for further studies due to its synthetic ease (in comparison to [Tb-**2**]$^-$), suitable quantum yield, little effect on cell viability, and modest cell association. Surprisingly, the addition of hydrophobic moieties (benzyl, hexyl, and trifluoro) did not increase cell association. All of the complexes investigated minimally affect cell viability and exhibit low cellular association, regardless of the overall complex charge or relative hydrophobicity; thus, it is presumed that it is the hydrophilic nature of the 2-methoxyisophthalamide antenna that confers the low membrane permeability of this class of compounds. Thus, the probes based on the structural framework presented here are well-suited for monitoring extracellular analytes such as group I ions, polysaccharides, hormones, or other signaling molecules.

EXPERIMENTAL SECTION

General Considerations. Unless otherwise noted, starting materials were obtained from commercial suppliers and used without further purification. Water was distilled and further purified by a Millipore cartridge system (resistivity 18 MΩ). Elemental analyses were performed by inductively coupled plasma mass spectrometry on a Thermo Scientific XSERIES 2 ICP-MS fitted with an ESI PC3 Peltier cooled spray chamber, SC-FAST injection loop, and SC-4 autosampler at the Department of Geology at the University of Minnesota. Samples were diluted appropriately and analyzed in the presence of a 20 ppb of In internal standard using the He/H2 collision-reaction mode. UV−vis spectra were measured with a Varian Cary 100 Bio spectrophotometer. Data were collected between 220 and 800 nm using a quartz cell with a path length of 10 mm. Luminescence data were recorded on a Varian Eclipse Fluorescence spectrophotometer using a quartz cell with a path length of 10 mm.

Determination of Quantum Yield (Φ). The absorbance and integrated luminescence intensities of [Tb-**1**]−[Tb-**3**] in PBS (pH 7.8, n = 1.3345) were compared to the reference fluorescence of quinine sulfate (Φ_r = 0.577)[16] in 0.1 M sulfuric acid (n = 1.333). Absorption spectra were collected on a Cary 100 Bio UV−visible spectrophotometer; emission spectra were recorded on a Cary Eclipse fluorescence spectrophotometer. Quantum yields (Φ) were calculated according to the optically dilute method using the equation

$$\Phi_x = \Phi_r\left(\frac{A_r}{A_x}\right)\left(\frac{n_x^2}{n_r^2}\right)\left(\frac{I_x}{I_r}\right)$$

where A is the absorbance at the excitation wavelength (λ), n is the refractive index, and I is the integrated intensity.[10c,d] The subscripts r and x refer to the reference and samples, respectively. All data were collected using the same spectrophotometer on the same day, resulting in a constant intensity of the excitation light (λ_{ex} = 350 nm). Measurements were obtained at 22 °C in a quartz cell of 1 cm path length in degassed solutions using an excitation wavelength of 350 nm and excitation and emission slit widths of 10 nm for both complexes. The fluorescence response of quinine sulfate was reported as the integrated emission intensity from 365 to 665 nm; the Tb luminescence of each complex was collected with a time delay of 0.1 ms and reported as the integrated emission intensity from 470 to 688 nm. The experiment was performed in triplicate (n = 3).

Cell Culture. Rat muscle L6 myoblast cell line was obtained from ATCC (Manassas, VA). Cells were cultured in 25 or 75 cm^2 vented culture flasks in Dulbecco's modified eagle medium (DMEM) supplemented with 10% (v/v) bovine serum (BS) and 10 μg of gentamicin mL^{-1} at 37 °C and 5% CO_2. The cells were maintained by splitting every 3−4 days before reaching confluence; cells were rinsed with PBS, lifted using 0.25 g L^{-1} typsin for 5 min, and diluted in fresh medium. All cells were propagated at low passage numbers (<20) to maintain their myoblastic character.

Preparation of Whole Cell Lysate. L6 cells were harvested from two 75 cm^2 culture flasks grown to 85% confluence and centrifuged at 400g for 10 min at 4 °C. The resulting pellet was rinsed with ice-cold PBS (2 mL) and centrifuged. The cells were then suspended in PBS (1 mL) and transferred to a tight-fitting homogenizer (B clearance 0.0008−0.0022 in.). Approximately 90% of the cells were ruptured after 120 strokes, as determined by cell counting with trypan blue and a hemocytometer. The total protein concentration of the whole cell lysate was determined with a bicinchoninic acid (BCA) assay (BCA Protein Assay Kit, ThermoScientific) using bovine serum albumin (BSA) protein standard solutions. The whole cell lysate was then diluted to a protein concentration of 1.0 mg/mL, and aliquots (450 μL) were stored at −20 °C for later use.

Luminescence Intensity in Whole Cell Lysate. An aqueous suspension of [Tb-**1**] (100 μM) in whole cell lysate diluted in PBS (0.25 or 0.5 mg of protein/mL) was titrated into an aqueous solution of whole cell lysate in PBS (0.25 or 0.5 mg of protein/mL). The time-delayed emission profile was recorded in the presence of 0−15 μM of Tb complex. The titration was repeated in pure PBS buffer (pH 7.8) without cell lysate. Measurements were recorded with an excitation wavelength of 345 nm, a time delay of 0.1 ms, and excitation and emission slit widths of 5 nm at a temperature of 20 °C. The luminescence response was reported as the integrated emission intensity from 470 to 640 nm. Each experiment was repeated in triplicate (n = 3). The percent quenching of the luminescence was calculated from the slopes of the integrated luminescence intensity versus the concentration of Tb complex (μM) plots in PBS and whole cell lysate at the two protein concentrations.

dx.doi.org/10.1021/ic500282n | Inorg. Chem. 2014, 53, 6013−6021

Cell Viability. L6 myoblasts (225 μL) were plated at ~4.0 × 10^4 cells mL^{-1} in a 48-well cell culture plate. Cells were allowed to recover 24 h, after which Tb complexes in PBS (25 μL) were added to the culture media (final concentrations of 0, 1, 3, 10, 30, 100, and 300 μM). For the negative control, PBS (without Tb complex) was used. The MTT assay was performed during the last 3 h of the compound exposure time as follows. MTT (3-(4,5-dimethylthiazolyl-2)-2,5-diphenyltetrazolium bromide, 25 μL of 5 mg/mL stock solution, 0.5 mg/mL final concentration) was added to the media, and the plate was returned to the cell culture incubator for 3 h. When a purple precipitate was clearly visible, 250 μL of 0.04 M HCl in isopropyl alcohol was added to each well. After an incubation of 4 h at room temperature in the dark, the samples were centrifuged at 10000*g* for 5 min to pellet cellular debris. For each sample, a portion of the supernatant (200 μL) was transferred to a corresponding well of a 96-well plate, and the absorbance at 570 and 690 nm was recorded using a microtiter plate reader. The cell viability was calculated according to the following equation using the adjusted absorbance of the cells treated with Tb complex in comparison to the control cells.[9a]

$$\text{viability}_{\text{MTT}}\ (\%) = \frac{(A_{570} - A_{690})_{\text{Tb complex}}}{(A_{570} - A_{690})_{\text{control}}}$$

Results are expressed as mean ± SD (n = 3).

Cellular Association by ICP-MS. The cellular association of [Tb-**1**]−[Tb-**10**] was investigated by seeding in triplicate L6 myoblasts (225 μL) at 4.5 × 10^4 cells mL^{-1} in a 48-well plate (~10000 cells mL^{-1}). Cells were allowed to recover for 48 h and had grown to 80% confluence, at which time a concentrated solution of Tb complex in PBS (25 μL) was added to achieve a final concentration of 50 μM in the cellular media. Cells grown in Tb complex free media (addition of only PBS) were included as a negative control. Following 4 h of incubation, the media were removed, and the wells were washed twice at room temperature by adding PBS and rocking the culture plate back and forth several times. The addition of a lysis buffer (75 μL of 10 mM Tris, pH 7.5, 100 mM NaCl, 1 mM Na_2EDTA, and 1% Triton X-100) followed by a 20 min incubation at 4 °C ruptured the cell membranes.[24] Aliquots (3 × 8 μL) from each well were removed for a BCA assay to determine the protein concentration. Samples (50 μL) were combined with concentrated nitric acid (50 μL) and heated to 95 °C for 18 h in flame-sealed glass ampules prior to ICP-MS analysis. The Tb content (ppb) was determined by ICP-MS, and the cellular association of each Tb complex (C_{Tb}), expressed as μmol of Tb/g of protein, was calculated according to the equation

$$C_{Tb} = (C_m/M)/C_p$$

where C_m is the measured metal concentration (ppb) of the cell samples, M is the molecular mass of Tb, and C_p is the protein concentration (mg/mL). Results are expressed as mean ± SD (n = 3).

Fluorescence Microscopy. L6 myoblasts (passage 9 or 10) were seeded in a polylysine-coated 8-well glass-bottom plate and allowed to grow for 24 h to 50% confluence at 37 °C in 5% CO_2. Then Tb complexes [Tb-**2**]$^-$−[Tb-**8**] were added in PBS for a final concentration of 200 μM. Negative control wells containing cells grown in Tb complex free media (addition of only PBS) were included. Following a 4 h incubation, the media were removed, and cells were washed three times with PBS at room temperature by rocking the culture plate back and forth gently. Cells were fixed with 4% formaldehyde in PBS at room temperature for 15 min. Additionally, live cell imaging of [Tb-**6**] was performed in DMEM phenol red free media. Epifluorescence images of representative cells were acquired on an Olympus IX81 inverted microscope equipped with a 60× (N.A. 1.45) oil immersion objective. Excitation was supplied by an Exfo XCite 120 metal halide lamp source coupled to the microscope via a liquid light guide, images were collected with a C9100−01 CCD camera, and HCImage software was utilized to control the microscope and camera and to process images. An excitation filter (325−375 nm), dichoric filter (460 nm), and emission filter (470−750 nm) were employed with exposure times of 0.4 s for fixed cells and 0.1 s for live cells. Bright field images of cells were also collected to determine the position of cells (exposure time 0.04 s). The contrast of bright field images was adjusted to a contrast range of 0−100 (normal range 0−255) using HCImage software.

■ ASSOCIATED CONTENT

Supporting Information

Text and figures giving synthetic details and characterization data for [Tb-**1**]−[Tb-**10**]$^{3-}$, time-delayed excitation and emission luminescence profiles, fluorescence emission profiles, and absorption spectra of [Tb-**1**]−[Tb-**3**], and supplementary fluorescence microscopy images of Tb complexes incubated with L6 myoblasts. This material is available free of charge via the Internet at http://pubs.acs.org.

■ AUTHOR INFORMATION

Corresponding Author

*E-mail for V.C.P.: pierre@umn.edu.

Notes

The authors declare no competing financial interest.

■ ACKNOWLEDGMENTS

We thank Edgar Arriaga, Michelle Henderson, and Greg Wolken for helpful discussions and assistance with cell culture and fluorescence microscopy and Rick Knurr for ICP-MS sample analysis. This work was supported by the National Science Foundation Grant CAREER 1151665. Support to K.L.P. from the NIH-CBITG (GM 08700), J.V.D. from the Heisig/Gleysteen Chemistry Summer Research Program from the Department of Chemistry at the University of Minnesota, E.A.W. through a Wayland E. Noland Fellowship from the Department of Chemistry at the University of Minnesota, and C.L. from a UROP fellowship from the University of Minnesota are gratefully acknowledged.

■ ABBREVIATIONS

ATP, adenosine triphosphate; BOC, *tert*-butoxycarbonyl; DIPEA, *N*,*N*-diisopropylethylamine; DMEM, Dulbecoo's modified eagle medium; DMF, dimethylformamide; DNA, DNA; DOTA, 1,4,7,10-tetraazacyclododecane-1,4,7,10-tetraacetic acid; DOTAm, 1,4,7,10-tetrakis(carbamoylmethyl)-1,4,7,10-tetraazacyclododecane; DTPA, diethylenetriaminepentaacetic acid; EDTA, ethylenediaminetetraacetic acid; Eu, europium; HATU, 1-[bis(dimethylamino)methylene]-1*H*-1,2,3-triazolo-[4,5-*b*]pyridinium 3-oxide hexafluorophosphate; IAM, 2-hydroxyisophthalamide; IAM(OMe), 2-methoxyisophthalamide; ED_{50}, half maximal effective dose; ICP-MS, Inductively coupled plasma mass spectrometry; Ir, iridium; Ln, lanthanide; MTT, (3-(4,5-dimethylthiazolyl-2)-2,5-diphenyltetrazolium bromide; PBS, phosphate buffered saline; PCC, pyridinium chlorochromate; Phen, 6-methylphenanthridine; Pt, platinum; Rh, rhodium; RNA, ribonucleic acid; ROS, reactive oxygen species; Ru, ruthenium; Tb, terbium

■ REFERENCES

(1) (a) Coogan, M. P.; Fernandez-Moreira, V. *Chem. Commun.* **2014**, *50*, 384−399. (b) Kobayashi, H.; Longmire, M. R.; Ogawa, M.; Choyke, P. L. *Chem. Soc. Rev.* **2011**, *40*, 4626−4648. (c) Lo, K. K.-W.; Choi, A. W.-T.; Law, W. H.-T. *Dalton Trans.* **2012**, *41*, 6021−6047. (d) Baggaley, E.; Weinstein, J. A.; Williams, J. A. G. *Coord. Chem. Rev.* **2012**, *256*, 1762−1785.

(2) (a) Thibon, A.; Pierre, V. C. *Anal. Bioanal. Chem.* **2009**, *394*, 107−120. (b) Bunzli, J. C. G.; Piguet, C. *Chem. Soc. Rev.* **2005**, *34*, 1048−1077.

(3) (a) Lippert, A. R.; Gschneidtner, T.; Chang, C. J. *Chem. Commun.* **2010**, *46*, 7510−7512. (b) Ye, Z.; Chen, J.; Wang, G.; Yuan, J. *Anal. Chem.* **2011**, *83*, 4163−4169. (c) Xiao, Y.; Ye, Z.; Wang, G.; Yuan, J. *Inorg. Chem.* **2012**, *51*, 2940−2946. (d) Peterson, K. L.; Margherio, M. J.; Doan, P.; Wilke, K. T.; Pierre, V. C. *Inorg. Chem.* **2013**, *52*, 9390−9398.
(4) (a) Kotova, O.; Comby, S.; Gunnlaugsson, T. *Chem. Commun.* **2011**, *47*, 6810−6812. (b) Comby, S.; Tuck, S. A.; Truman, L. K.; Kotova, O.; Gunnlaugsson, T. *Inorg. Chem.* **2012**, *51*, 10158−10168.
(5) (a) Moore, J. D.; Lord, R. L.; Cisneros, G. A.; Allen, M. J. *J. Am. Chem. Soc.* **2012**, *134*, 17372−17375. (b) McMahon, B. K.; Pal, R.; Parker, D. *Chem. Commun.* **2013**, *49*, 5363−5365.
(6) Weitz, E. A.; Chang, J. Y.; Rosenfield, A. H.; Pierre, V. C. *J. Am. Chem. Soc.* **2012**, *134*, 16099−16102.
(7) (a) Puckett, C. A.; Barton, J. K. *J. Am. Chem. Soc.* **2007**, *129*, 46−47. (b) Weidmann, A. G.; Komor, A. C.; Barton, J. K. *Philos. Trans. R. Soc. A* **2013**, *371*, 20120117−20120117. (c) Chauvin, A.-S.; Thomas, F.; Song, B.; Vandevyver, C. D. B.; Bunzli, J.-C. G. *Philos. Trans. R. Soc. A* **2013**, *371*, 20120295−20120295. (d) New, E. J.; Congreve, A.; Parker, D. *Chem. Sci.* **2010**, *1*, 111−118. (e) Murray, B. S.; New, E. J.; Pal, R.; Parker, D. *Org. Biomol. Chem.* **2008**, *6*, 2085−2094.
(8) (a) Major, J. L.; Meade, T. J. *Acc. Chem. Res.* **2009**, *42*, 893−903. (b) Vithanarachchi, S. M.; Allen, M. J. *Curr. Mol. Imaging* **2012**, *1*, 12−25.
(9) (a) Song, B.; Vandevyver, C. D.; Chauvin, A. S.; Bunzli, J. C. *Org. Biomol. Chem.* **2008**, *6*, 4125−4133. (b) Parker, D. *Aust. J. Chem.* **2011**, *64*, 239−243. (c) New, E. J.; Parker, D.; Smith, D. G.; Walton, J. W. *Curr. Opin. Chem. Biol.* **2010**, *14*, 238−246.
(10) (a) Weitz, E. A.; Chang, J. Y.; Rosenfield, A. H.; Morrow, E. A.; Pierre, V. C. *Chem. Sci.* **2013**, *4*, 4052−4060. (b) Smolensky, E. D.; Peterson, K. L.; Weitz, E. A.; Lewandowski, C.; Pierre, V. C. *J. Am. Chem. Soc.* **2013**, *135*, 8966−8972. (c) Law, G.-L.; Pham, T. A.; Xu, J.; Raymond, K. N. *Angew. Chem., Int. Ed.* **2012**, *51*, 2371−2374. (d) Samuel, A. P. S.; Moore, E. G.; Melchior, M.; Xu, J.; Raymond, K. N. *Inorg. Chem.* **2008**, *47*, 7535−7544.
(11) Cacheris, W. P.; Quay, S. C.; Rocklage, S. M. *Magn. Reson. Imaging* **1990**, *8*, 467−481.
(12) Hermann, P.; Kotek, J.; Kubicek, V.; Lukes, I. *Dalton Trans.* **2008**, 3027−3047.
(13) Di Gregorio, E.; Gianolio, E.; Stefania, R.; Barutello, G.; Digilio, G.; Aime, S. *Anal. Chem.* **2013**, *85*, 5627−5631.
(14) (a) Woods, M.; Kiefer, G. E.; Bott, S.; Castillo-Muzquiz, A.; Eshelbrenner, C.; Michaudet, L.; McMillan, K.; Mudigunda, S. D. K.; Ogrin, D.; Tircsó, G.; Zhang, S.; Zhao, P.; Sherry, A. D. *J. Am. Chem. Soc.* **2004**, *126*, 9248−9256. (b) Jeon, J. W.; Son, S. J.; Yoo, C. E.; Hong, I. S.; Song, J. B.; Suh, J. *Org. Lett.* **2002**, *4*, 4155−4158.
(15) (a) Moreau, J.; Guillon, E.; Pierrard, J. C.; Rimbault, J.; Port, M.; Aplincourt, M. *Chem. Eur. J.* **2004**, *10*, 5218−5232. (b) Lattuada, L.; Barge, A.; Cravotto, G.; Giovenzana, G. B.; Tei, L. *Chem. Soc. Rev.* **2011**, *40*, 3019−3049.
(16) Lakowicz, J. R. *Principles of Fluorescence Spectroscopy*, 3rd ed.; Springer: Singapore, 2006.
(17) Parker, D.; Senanayake, P. K.; Williams, J. A. G. *J. Chem. Soc., Perkin Trans. 2* **1998**, 2129−2139.
(18) Li, C.; Liu, Y.; Wu, Y.; Sun, Y.; Li, F. *Biomaterials* **2013**, *34*, 1223−1234.
(19) Resch-Genger, U.; Grabolle, M.; Cavaliere-Jaricot, S.; Nitschke, R.; Nann, T. *Nat. Methods* **2008**, *5*, 763−775.
(20) Fernandez-Moreira, V.; Thorp-Greenwood, F. L.; Coogan, M. P. *Chem. Commun.* **2010**, *46*, 186−202.
(21) (a) Poole, R. A.; Montgomery, C. P.; New, E. J.; Congreve, A.; Parker, D.; Botta, M. *Org. Biomol. Chem.* **2007**, *5*, 2055−2062. (b) Kielar, F.; Montgomery, C. P.; New, E. J.; Parker, D.; Poole, R. A.; Richardson, S. L.; Stenson, P. A. *Org. Biomol. Chem.* **2007**, *5*, 2975−2982.
(22) Kielar, F.; Law, G.-L.; New, E. J.; Parker, D. *Org. Biomol. Chem.* **2008**, *6*, 2256−2258.
(23) Weitz, E. A.; Chang, J. Y.; Rosenfield, A. H.; Pierre, V. C. *J. Am. Chem. Soc.* **2012**, *134*, 16099−16102.
(24) New, E. J.; Parker, D. *Org. Biomol. Chem.* **2009**, *7*, 851−855.
(25) Dosio, F.; Stella, B.; Ferrero, A.; Garino, C.; Zonari, D.; Arpicco, S.; Cattel, L.; Giordano, S.; Gobetto, R. *Int. J. Pharm.* **2013**, *440*, 221−228.
(26) Darghal, N.; Garnier-Suillerot, A.; Bouchemal, N.; Gras, G.; Geraldes, C. F. G. C.; Salerno, M. *J. Inorg. Biochem.* **2010**, *104*, 47−54.
(27) Puckett, C. A.; Ernst, R. J.; Barton, J. K. *Dalton Trans.* **2010**, *39*, 1159−1170.
(28) Park, G. Y.; Wilson, J. J.; Song, Y.; Lippard, S. J. *Proc. Natl. Acad. Sci. U.S.A.* **2012**, *109*, 11987−11992.
(29) (a) Puckett, C. A.; Barton, J. K. *Biochemistry* **2008**, *47*, 11711−11716. (b) Lo, K. K.-W.; Lee, P.-K.; Lau, J. S.-Y. *Organometallics* **2008**, *27*, 2998−3006.
(30) (a) Walton, J. W.; Bourdolle, A.; Butler, S. J.; Soulie, M.; Delbianco, M.; McMahon, B. K.; Pal, R.; Puschmann, H.; Zwier, J. M.; Lamarque, L.; Maury, O.; Andraud, C.; Parker, D. *Chem. Commun.* **2013**, *49*, 1600−1602. (b) Lee, P.-K.; Law, W. H.-T.; Liu, H.-W.; Lo, K. K.-W. *Inorg. Chem.* **2011**, *50*, 8570−8579.
(31) Zhao, Q.; Huang, C.; Li, F. *Chem. Soc. Rev.* **2011**, *40*, 2508−2524.
(32) Stewart, K. M.; Horton, K. L.; Kelley, S. O. *Org. Biomol. Chem.* **2008**, *6*, 2242−2255.
(33) Gianolio, E.; Stefania, R.; Di Gregorio, E.; Aime, S. *Eur. J. Inorg. Chem.* **2012**, 1934−1944.
(34) (a) Allen, M. J.; MacRenaris, K. W.; Venkatasubramanian, P. N.; Meade, T. J. *Chem. Biol.* **2004**, *11*, 301−307. (b) Allen, M. J.; Meade, T. J. *J. Biol. Inorg. Chem.* **2003**, *8*, 746−750. (c) Endres, P. J.; MacRenaris, K. W.; Vogt, S.; Allen, M. J.; Meade, T. J. *Mol. Imag.* **2006**, *5*, 485−497. (d) Futaki, S.; Goto, S.; Sugiura, Y. *J. Mol. Recognit.* **2003**, *16*, 260−264. (e) Que, E. L.; New, E. J.; Chang, C. J. *Chem. Sci.* **2012**, *3*, 1829−1834.
(35) Bhorade, R.; Weissleder, R.; Nakakoshi, T.; Moore, A.; Tung, C. H. *Bioconjugate Chem.* **2000**, *11*, 301−305.
(36) (a) Mohandessi, S.; Rajendran, M.; Magda, D.; Miller, L. W. *Chem. Eur. J.* **2012**, *18*, 10825−10829. (b) Blackmore, L.; Moriarty, R.; Dolan, C.; Adamson, K.; Forster, R. J.; Devocelle, M.; Keyes, T. E. *Chem. Commun.* **2013**, *49*, 2658−2660. (c) Puckett, C. A.; Barton, J. K. *Bioorg. Med. Chem.* **2010**, *18*, 3564−3569.
(37) Keliris, A.; Ziegler, T.; Mishra, R.; Pohmann, R.; Sauer, M. G.; Ugurbil, K.; Engelmann, J. *Bioorg. Med. Chem.* **2011**, *19*, 2529−2540.
(38) (a) Wolf, M.; Hull, W. E.; Mier, W.; Heiland, S.; Bauder-Wuest, U.; Kinscherf, R.; Haberkorn, U.; Eisenhut, M. *J. Med. Chem.* **2007**, *50*, 139−148. (b) Lee, J.; Burclette, J. E.; MacRenaris, K. W.; Mustafi, D.; Woodruff, T. K.; Meade, T. J. *Chem. Biol.* **2007**, *14*, 824−834. (c) Corot, C.; Robert, P.; Lancelot, E.; Prigent, P.; Ballet, S.; Guilbert, I.; Raynaud, J.-S.; Raynal, I.; Port, M. *Magn. Reson. Med.* **2008**, *60*, 1337−1346. (d) Goswami, L. N.; Ma, L.; Cai, Q.; Sarma, S. J.; Jalisatgi, S. S.; Hawthorne, M. F. *Inorg. Chem.* **2013**, *52*, 1701−1709. (e) Andre, J. P.; Geraldes, C.; Martins, J. A.; Merbach, A. E.; Prata, M. I. M.; Santos, A. C.; de Lima, J. J. P.; Toth, E. *Chem. Eur. J.* **2004**, *10*, 5804−5816.
(39) Crich, S. G.; Cabella, C.; Barge, A.; Belfiore, S.; Ghirelli, C.; Lattuada, L.; Lanzardo, S.; Mortillaro, A.; Tei, L.; Visigalli, M.; Forni, G.; Aime, S. *J. Med. Chem.* **2006**, *49*, 4926−4936.
(40) Digilio, G.; Menchise, V.; Gianolio, E.; Catanzaro, V.; Carrera, C.; Napolitano, R.; Fedeli, F.; Aime, S. *J. Med. Chem.* **2010**, *53*, 4877−4890.
(41) Belitsky, J. M.; Leslie, S. J.; Arora, P. S.; Beerman, T. A.; Dervan, P. B. *Bioorg. Med. Chem.* **2002**, *10*, 3313−3318.